Journal of Solid State Chemistry 184 (2011) 1367–1372

Contents lists available at ScienceDirect

Journal of Solid State Chemistry

journal homepage: www.elsevier.com/locate/jssc

NMR relaxation study of the phase transitions and relaxation mechanisms of the alums $M\mathrm{Cr}(\mathrm{SO_4})_2\cdot 12\mathrm{H_2O}$ (M=Rb and Cs) single crystals

Ae Ran Lim [a,*], Younkee Paik [b], Kye-Young Lim [c]

[a] Department of Science Education, Jeonju University, Jeonju 560-759, Republic of Korea
[b] Solid State Analysis Team, Korea Basic Science Institute, Daegu 702-701, Republic of Korea
[c] Department of Energy & Electrical Engineering, Korea Polytechnic University, Siheung 429-793, Republic of Korea

ARTICLE INFO

Article history:
Received 13 July 2010
Received in revised form
13 February 2011
Accepted 4 April 2011
Available online 13 April 2011

Keywords:
Alums
$\mathrm{CsCr(SO_4)_2\cdot 12H_2O}$
$\mathrm{RbCr(SO_4)_2\cdot 12H_2O}$
Phase transformations
Nuclear magnetic resonance (NMR)

ABSTRACT

The physical properties and phase transition mechanisms of $M\mathrm{Cr(SO_4)_2\cdot 12H_2O}$ (M=Rb and Cs) single crystals have been investigated. The phase transition temperatures, NMR spectra, and the spin-lattice relaxation times T_1 of the ^{87}Rb and ^{133}Cs nuclei in the two crystals were determined using DSC and FT NMR spectroscopy. The resonance lines and relaxation times of the ^{87}Rb and ^{133}Cs nuclei undergo significant changes at the phase transition temperatures. The sudden changes in the splitting of the Rb and Cs resonance lines are attributed to changes in the local symmetry of their sites, and the changes in the temperature dependences of T_1 are related to variations in the symmetry of the octahedra of water molecules surrounding $\mathrm{Rb^+}$ and $\mathrm{Cs^+}$. We also compared these ^{87}Rb and ^{133}Cs NMR results with those obtained for the trivalent cations Cr and Al in $M\mathrm{Cr(SO_4)_2\cdot 12H_2O}$ and $M\mathrm{Al(SO_4)_2\cdot 12H_2O}$ crystals.

1. Introduction

The alums can be represented with the general formula $M^+Me^{3+}(\mathrm{SO_4})_2\cdot 12\mathrm{H_2O}$, where M is a monovalent cation such as Na, K, Rb, Cs, or $\mathrm{NH_4}$, and Me is a trivalent cation such as Al, Fe, or Cr [1,2]. The alums investigated in this study were $M^+Me^{3+}(\mathrm{SO_4})_2\cdot 12\mathrm{H_2O}$ (M=Rb, Cs and Me=Cr, Al). Alums are classified as α, β, or γ, which correspond to three slightly different arrangements of the ions and molecules within the cubic lattice [3]. Common to the three subtypes is the arrangement of the M^+ and Me^{3+} ions, which form a cubic face-centered lattice. M^+ and Me^{3+} ions are each surrounded by six $\mathrm{H_2O}$ molecules. The Me^{3+} ions are surrounded by almost regular octahedra of $\mathrm{H_2O}$. The orientation of this octahedron with respect to the crystal axes is slightly different for α-, β-, and γ-alums [4]. If the M cation is small, a γ-alum forms. The only known representative of this class is $\mathrm{NaCr(SO_4)_2\cdot 12H_2O}$. A β-alum forms if the M cation is large, such as in $\mathrm{CsCr(SO_4)_2\cdot 12H_2O}$, and an α-alum, which is by far the most common type, forms if the M cation is medium, such as in $\mathrm{KCr(SO_4)_2\cdot 12H_2O}$, $\mathrm{RbCr(SO_4)_2\cdot 12H_2O}$, and $\mathrm{NH_4Cr(SO_4)_2\cdot 12H_2O}$ [5,6]. The $M^+(\mathrm{H_2O})_6$ octahedra in γ-alums are quite regular. In the α-alums, the $M^+(\mathrm{H_2O})_6$ octahedra are distorted by a flattening parallel to one of the threefold axes, and in the β-alums the distortion leads to an almost planar arrangement of the six $\mathrm{H_2O}$ molecules around the central ion M^+.

The phase transition temperatures of $\mathrm{RbCr(SO_4)_2\cdot 12H_2O}$ and $\mathrm{CsCr(SO_4)_2\cdot 12H_2O}$ crystals have not previously been established. A variety of salts with interesting properties have been studied with many methods in recent years. Some questions, however, have not yet been resolved, especially those related to the nature of their phase transitions. The connection between the crystal structures and the thermal stabilities of the alums has been discussed by Cudey [7]. The quadrupole coupling constants of ^{87}Rb and ^{133}Cs in $M\mathrm{Cr(SO_4)_2\cdot 12H_2O}$ and $M\mathrm{Al(SO_4)_2\cdot 12H_2O}$ (M=Rb and Cs) crystals have been reported using the static nuclear magnetic resonance (NMR) method by Weiden and Weiss [8,9]; in the cases of $\mathrm{RbCr(SO_4)_2\cdot 12H_2O}$ and $\mathrm{RbAl(SO_4)_2\cdot 12H_2O}$, the quadrupole coupling constants of the ^{87}Rb nucleus were found to be 12.735 and 13.221 MHz, respectively, and the quadrupole coupling constant of the ^{133}Cs nucleus in $\mathrm{CsAl(SO_4)_2\cdot 12H_2O}$ was found to be 229.5 kHz. Although the electron paramagnetic resonance (EPR) and NMR studies of $M\mathrm{Al(SO_4)_2\cdot 12H_2O}$ (M=Rb and Cs) at room temperature have been carried out [10–18], the physical properties and phase transition temperatures of $M\mathrm{Cr(SO_4)_2\cdot 12H_2O}$ (M=Rb and Cs) single crystals have not yet been reported.

In the present study, the NMR spectra and spin-lattice relaxation times, T_1, for ^{87}Rb and ^{133}Cs nuclei in $\mathrm{RbCr(SO_4)_2\cdot 12H_2O}$ and $\mathrm{CsCr(SO_4)_2\cdot 12H_2O}$ single crystals were obtained. In addition, we investigated the phase transitions of these crystals using

* Corresponding author. Fax: +82 0 63 220 2053.
E-mail addresses: aeranlim@hanmail.net, arlim@jj.ac.kr (A. Ran Lim).

0022-4596/$ - see front matter © 2011 Elsevier Inc. All rights reserved.
doi:10.1016/j.jssc.2011.04.009

differential scanning calorimetry (DSC), thermogravimetric analysis (TGA), optical polarizing microscopy, and NMR. To probe the phase transitions that occur in the two single crystals, the measurement of the ^{87}Rb and ^{133}Cs relaxation times was preferred, because the ^{87}Rb and ^{133}Cs relaxation times are likely to be very sensitive to changes in the symmetry of these crystals. This is the first time that the phase transitions of $RbCr(SO_4)_2 \cdot 12H_2O$ and $CsCr(SO_4)_2 \cdot 12H_2O$ crystals have been investigated, and we use these results to analyze the environments of the Rb and Cs nuclei. We also compare our results for $MCr(SO_4)_2 \cdot 12H_2O$ (M=Rb and Cs) with those for $MAl(SO_4)_2 \cdot 12H_2O$ crystals, which have a similar structure. The comparison of the effects of Cr and Al on their respective alum crystals is an interesting area of study. Therefore, this work significantly enhances understanding of the relaxation processes and the nature of phase transitions occurring in these crystals.

2. Crystal structure

The structures of $MCr(SO_4)_2 \cdot 12H_2O$ (M=Rb and Cs) crystals have previously been determined using X-ray diffraction [19–21]. These single crystals have cubic structures and belong to the space group $Pa\bar{3}$, with four molecules per unit cell. The lattice parameters of $RbCr(SO_4)_2 \cdot 12H_2O$ and $CsCr(SO_4)_2 \cdot 12H_2O$ crystals are $a=b=c=12.296$ and 12.352 Å, respectively. The M^+ and Cr^{3+} ions in $MCr(SO_4)_2 \cdot 12H_2O$ crystals are each surrounded by six water molecules, as shown in Fig. 1 [19]. The nearest neighbors of Cr^{3+} are six water molecules, which form a nearly regular octahedron. In contrast, the octahedron of water molecules about M^+ is strongly distorted.

3. Experimental method

The $MCr(SO_4)_2 \cdot 12H_2O$ (M=Rb and Cs) single crystals were prepared by the slow evaporation of aqueous solutions at 293 K. The $MCr(SO_4)_2 \cdot 12H_2O$ specimens are hexagonal with dimensions of $4 \times 4 \times 3$ mm^3.

The structures of $RbCr(SO_4)_2 \cdot 12H_2O$ and $CsCr(SO_4)_2 \cdot 12H_2O$ single crystals at room temperature were determined with an X-ray diffractometer system (Bruker AXS GMBH) at the Korea Basic Science Institute. And, in order to determine the phase transition temperatures, DSC was carried out on the crystals using a Dupont 2010 DSC instrument. Measurements were made at a heating rate of 10 °C/min. TGA was carried out on the crystals using a Sinco TGA-1000 instrument. In addition, the NMR measurements for the ^{87}Rb and ^{133}Cs nuclei in the $MCr(SO_4)_2 \cdot 12H_2O$ single crystals were obtained with the 400 FT NMR spectroscopy at the Korea Basic Science Institute. The static magnetic field was 9.4 T, and the central radio frequency was set at $\omega_0/2\pi=130.90$ MHz for the ^{87}Rb nucleus and at $\omega_0/2\pi=52.48$ MHz for the ^{133}Cs nucleus. The spin-lattice relaxation times were measured using a saturation recovery pulse sequence, sat–t–$\pi/2$: the nuclear magnetizations of the ^{87}Rb and ^{133}Cs nuclei at time t after the sat pulse, a comb of one hundred of $\pi/2$ pulses applied at a regular interval of 10 μs, were determined following the excitation $\pi/2$ pulse. The widths of the $\pi/2$ pulses were 1 s for ^{87}Rb and 1.65 μs for ^{133}Cs. The temperature-dependent NMR measurements were carried out over the temperature range 180–420 K. The samples were maintained at constant temperatures by controlling the nitrogen gas flow and the heater current. The temperature controller was calibrated using the temperature dependence of the chemical shift of ^{207}Pb nucleus in $Pb(NO_3)_2$ at a temperature range 150–500 K [22]. The precision of the sample temperature was within ±1 K at the experimental range 180–420 K.

4. Experimental results and analysis

4.1. ^{87}Rb NMR for $RbCr(SO_4)_2 \cdot 12H_2O$ single crystals

From our X-ray diffraction result, the structure of a $RbCr(SO_4)_2 \cdot 12H_2O$ crystal was found to have cubic symmetry with cell parameters $a=b=c=12.278$ Å. This result is consistent with that of Figgis et al. [19]. Optical polarizing microscopy was used to show that the color of these crystals varies with temperature: dark purple at room temperature, light purple near 400 K, and dark green near 460 K. This variation in color might be related to the loss of H_2O. Two endothermic peaks were found with DSC for $RbCr(SO_4)_2 \cdot 12H_2O$ at 374 and 425 K, as shown in Fig. 2. TGA was used to determine whether the high-temperature transformations are structural phase transitions or chemical reactions. The thermogram of $RbCr(SO_4)_2 \cdot 12H_2O$ is shown in the inset in Fig. 2. The mass loss begins in the vicinity of 330 K, and transformation at 330 K ($=T_d$) is due to the onset of partial thermal decomposition. Also, we checked for premelting with optical polarizing microscopy. We conclude that the endothermic peaks at 374 K (T_{C1}) and 425 K (T_{C2}) correspond to phase transitions.

The NMR spectrum of ^{87}Rb ($I=3/2$) in $RbCr(SO_4)_2 \cdot 12H_2O$ was obtained at a frequency of $\omega_0/2\pi=130.90$ MHz. When such crystals are rotated about the crystallographic axis, the crystallographically equivalent nuclei would be expected to give rise to three lines: one central line and two satellite lines. Instead of one central resonance line, four central resonance lines were obtained for the $RbCr(SO_4)_2 \cdot 12H_2O$ crystal. The signals were obtained with the magnetic field applied along the crystallographic c-axis.

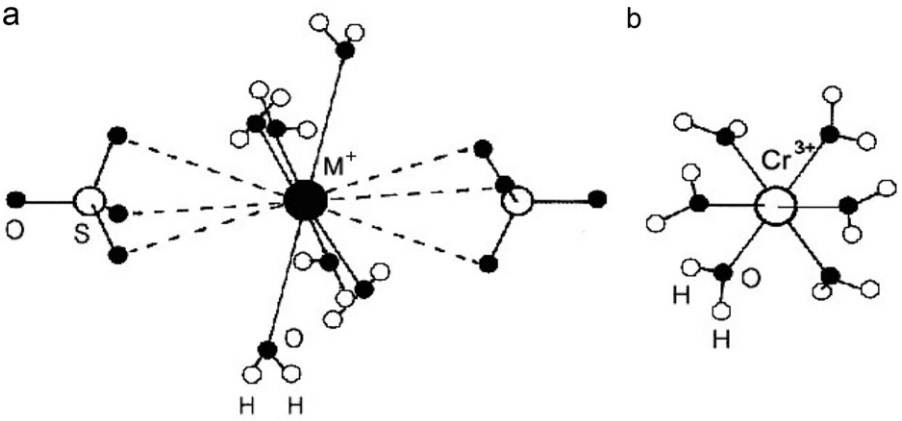

Fig. 1. Environments of (a) M^+ and (b) Cr^{3+} in $MCr(SO_4)_2 \cdot 12H_2O$ (M=Rb and Cs) at room temperature.

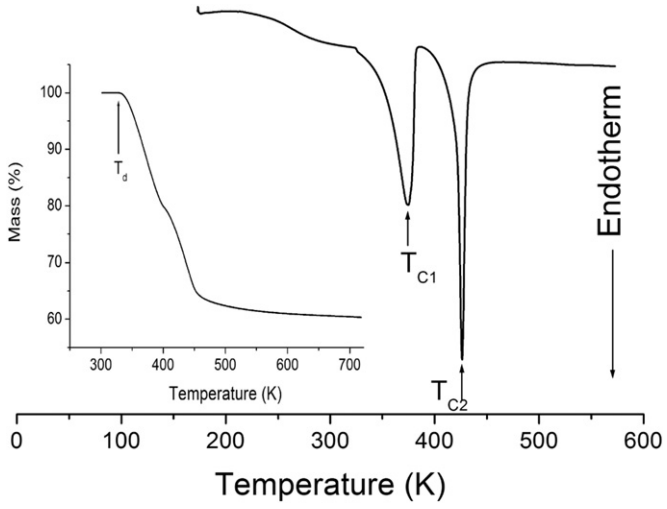

Fig. 2. Differential scanning calorimetry (DSC) thermogram for $RbCr(SO_4)_2 \cdot 12H_2O$ crystals (inset: thermogravimetry analysis (TGA) for $RbCr(SO_4)_2 \cdot 12H_2O$ crystals).

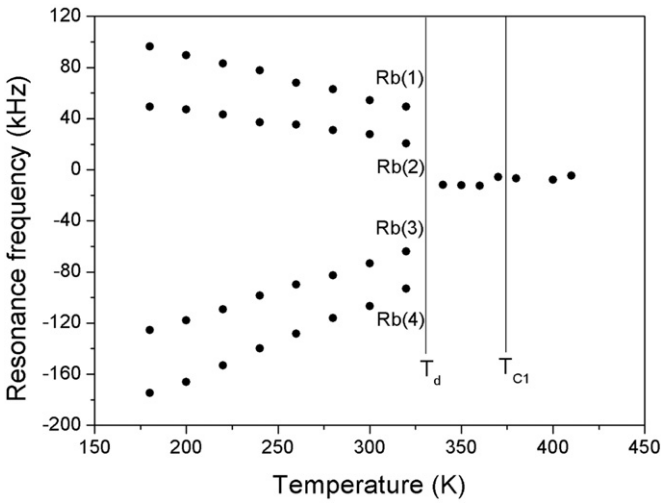

Fig. 3. Separation of the Rb resonance lines as a function of temperature.

In this figure, the zero point of the frequency axis is set to the resonance frequency, 130.90 MHz, of the ^{87}Rb nucleus. Over the temperature range 180–420 K, the whole spectrum is shifted by the paramagnetic ion. The Rb resonance lines are displaced to lower frequencies by the paramagnetic ions relative to the reference signal of the ^{87}Rb resonance line for an aqueous solution of RbCl. The shifts in the resonance lines of $RbCr(SO_4)_2 \cdot 12H_2O$ might be due to dipole–dipole interactions between the magnetic moments of the Rb^+ nuclei and the magnetic moments of the Cr^{3+} atoms. The magnitudes of the quadrupole parameters of the ^{87}Rb nucleus are of the order of MHz as previously reported [8,9], so usually only central line is obtained. The satellite resonance lines for the ^{87}Rb nucleus correspond to transitions between the levels $(+3/2 \leftrightarrow +1/2)$ and $(-1/2 \leftrightarrow -3/2)$, and lie outside the frequency range of the NMR probe. Thus, the four resonance lines are for the central transition of the ^{87}Rb NMR spectrum. Larson and Cromer [23] have reported that the Rb nuclei in the crystal structure are crystallographically equivalent. From these results, we think that four types of magnetically inequivalent sites, Rb(1), Rb(2), Rb(3), and Rb(4) nuclei exist in the unit cell. This result is consistent with four Rb resonance lines in $RbAl(SO_4)_2 \cdot 12H_2O$ crystals previously reported [24]. The spacing between the resonance lines decreases with increasing temperature. Further, there is only one ^{87}Rb resonance line above 330 K, as shown in Fig. 3. Above T_d (=330 K), which is about 45 K lower than the phase transition temperature 374 K (T_{C1}), the presence of only one ^{87}Rb resonance line is associated with the structural phase transition. The change of Rb resonance lines near 330 K is related to the loss of H_2O, as found in the TGA result; the forms of the octahedra of water molecules surrounding Rb^+ are probably disrupted by the loss of H_2O. This sudden change in the splitting of the Rb resonance line is due to changes in the local symmetry of the ^{87}Rb sites. On the other hand, in the present study the spectrum could not be determined above 420 K because the NMR spectrometer did not have adequate temperature control at high temperatures; hence, the phase transition at 425 K could not be detected in the ^{87}Rb NMR results. The changes in the line positions indicate that the electric field gradient (EFG) at the ^{87}Rb sites varies with temperature, which in turn indicates that the atoms neighboring the ^{87}Rb atoms are displaced at high temperatures.

The variations of the nuclear magnetization of ^{87}Rb in $RbCr(SO_4)_2 \cdot 12H_2O$ with delay time were measured at several temperatures. When only the central transition is considered, the recovery law for quadrupole relaxation in ^{87}Rb nuclear spin systems can be represented by a combination of two exponential functions [25,26]:

$$[S(\infty)-S(t)]/S(\infty) = 0.5\exp(-2W_1t)+0.5\exp(-2W_2t) \quad (1)$$

where W_1 and W_2 are the transition probabilities corresponding to the $\Delta m = \pm 1$ and $\Delta m = \pm 2$ transitions, respectively, and $S(t)$ is the nuclear magnetization corresponding to the central transition at time t after saturation. The spin-lattice relaxation time is given by [25–27]

$$T_1 = 5/[2(W_1+4W_2)] \quad (2)$$

It is well known that a relaxation time T_1 can only be defined if the time dependence of the magnetization can be described with a single exponential relaxation function. Of course, one can introduce a useful combination of the transition probabilities W_1 and W_2 according to Eq. (2); the introduction of this constant would be reasonable because it leads to the correct relaxation time $T_1 = 1/2W_1$ in the case of $W_1 = W_2$, and then from Eq. (1) a single exponential relaxation function can be derived.

The recovery trace for the central line of ^{87}Rb ($I=3/2$) with dominant quadrupole relaxation can be represented by a combination of two exponential functions. Here, W_1 and W_2 have the same values in the recovery traces of ^{87}Rb nuclei at all temperatures in the range we examined. Therefore, these results can be discussed in terms of a relaxation time T_1 according to $T_1 = 1/2W_1$. We determined the variations with temperature of the relaxation times for the central resonance lines of the Rb nuclei. The temperature dependences of the ^{87}Rb spin-lattice relaxation time, T_1, are shown in Fig. 4. Here, the T_1 values for the four Rb nuclei are similar. The T_1 of the ^{87}Rb nuclei were found to undergo significant changes near T_{C1}, and these changes coincide with the changes in the splitting of the ^{87}Rb resonance lines. The Rb T_1 is very short, on the order of milliseconds. The abrupt change in T_1 at T_{C1} is the only detectable result of the structural transformation.

4.2. ^{133}Cs NMR in $CsCr(SO_4)_2 \cdot 12H_2O$ single crystals

The structure of the $CsCr(SO_4)_2 \cdot 12H_2O$ single crystals at room temperature was determined; these crystals have cubic symmetry with cell parameters $a=b=c=12.390$ Å. This result is consistent with that of Best and Forsyth [20]. An endothermic peak by DSC results was found at 390 K for $CsCr(SO_4)_2 \cdot 12H_2O$, as shown in Fig. 5, which indicates that this crystal undergoes a phase transition at this temperature. And, the mass loss begins near 360 K (see inset in

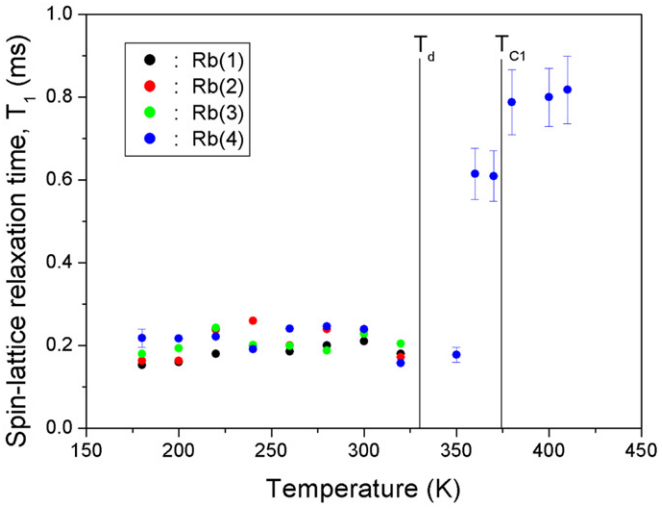

Fig. 4. Temperature dependences of the spin-lattice relaxation time, T_1, of ^{87}Rb nuclei in a $RbCr(SO_4)_2 \cdot 12H_2O$ single crystal.

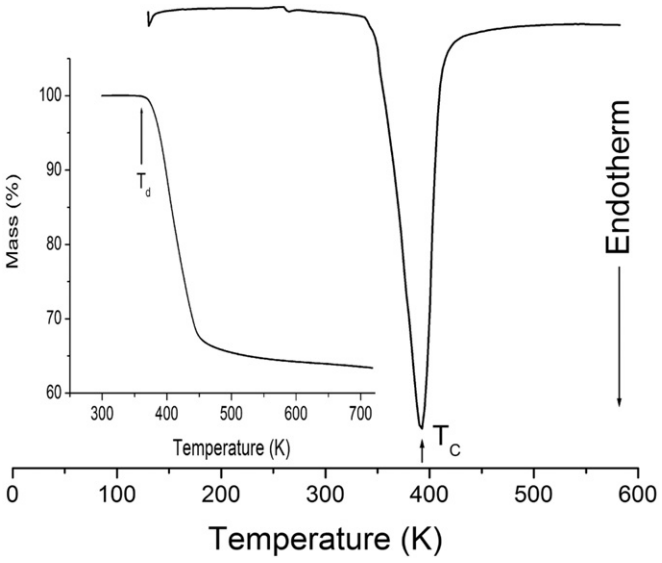

Fig. 5. The differential scanning calorimetry (DSC) thermogram for $CsCr(SO_4)_2 \cdot 12H_2O$ crystals (inset: thermogravimetry analysis (TGA) for $CsCr(SO_4)_2 \cdot 12H_2O$ crystals).

Fig. 5), which is interpreted as the onset of partial thermal decomposition. Optical polarizing microscopy was used to show that the color of this crystal varies with temperature: dark blue at room temperature and light blue near 420 K. This variation in color might be related to the loss of H_2O.

The NMR spectrum of ^{133}Cs ($I=7/2$) was obtained at several temperatures. Seven resonance lines were observed when the magnetic field was applied along the crystallographic *c*-axis. The central transition is almost unshifted by the quadrupole interaction, and the resonance line splitting between the satellite lines varies with temperature. Further, the Cs resonance lines are displaced to lower frequencies by the paramagnetic shift relative to the reference signal of the ^{133}Cs resonance line of an aqueous solution of $CsCl_3$. The paramagnetic shifts of the Cs signals for $CsCr(SO_4)_2 \cdot 12H_2O$ single crystals are shown as functions of temperature in Fig. 6(a). The shift of the resonance lines of $CsCr(SO_4)_2 \cdot 12H_2O$ is related to the transferred hyperfine interaction of the Cr^{3+} ions. The variation in the splitting of the ^{133}Cs resonance lines with temperature indicates that the electric field gradient (EFG) at the Cs sites varies with temperature, which in turn means that the displacements of the atoms neighboring ^{133}Cs

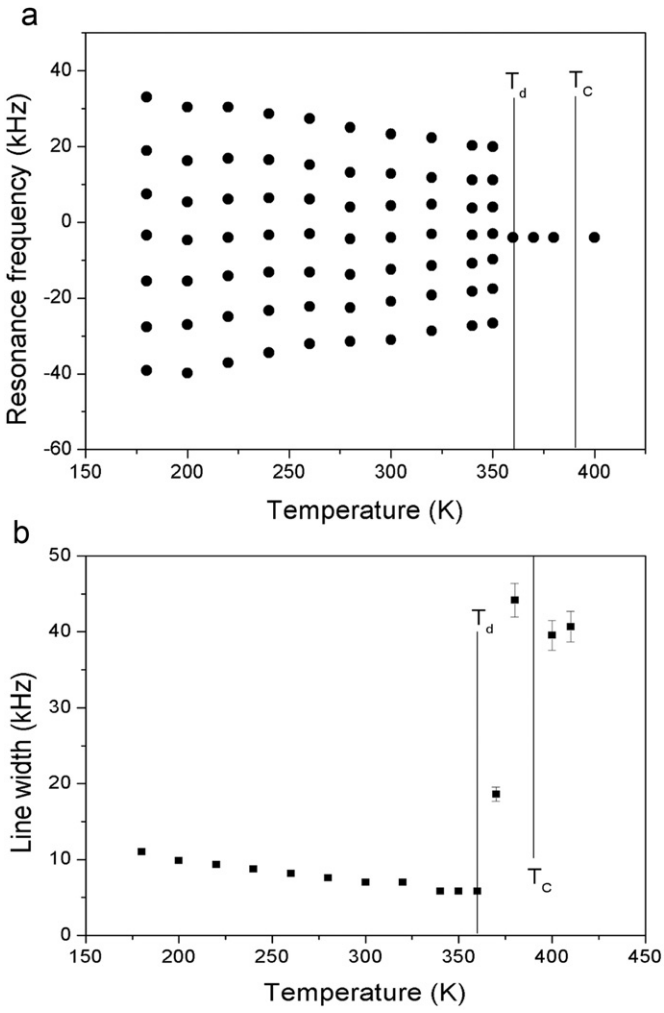

Fig. 6. (a) Separation of the Cs resonance lines as a function of temperature and (b) the line widths for the ^{133}Cs nucleus in $CsCr(SO_4)_2 \cdot 12H_2O$ crystals as functions of temperature.

vary with temperature. Above 360 K (T_d), the presence of only one ^{133}Cs resonance line indicates that the electric quadrupole moments of the ^{133}Cs nucleus cause no perturbation of the eight nuclear Zeeman levels. The change of Cs resonance lines near 360 K is related to the loss of H_2O, as found in the TGA result. This result means that the symmetry of the Cs sites in $CsCr(SO_4)_2 \cdot 12H_2O$ is cubic; the octahedron of water molecules surrounding Cs^+ is symmetrical above T_C. Further, the line-width for the central resonance line of the ^{133}Cs nucleus in the $CsCr(SO_4)_2 \cdot 12H_2O$ crystals is shown as a function of temperature in Fig. 6(b). The line-width is nearly constant with increasing temperature, and abruptly increases at the phase transition temperature of 390 K. The abrupt change in the line-width is due to the increasing of the quadrupolar broadening.

When only the central line is excited, the magnetization recovery of the ^{133}Cs nucleus in the $CsCr(SO_4)_2 \cdot 12H_2O$ crystal does not follow a single exponential function, but can be represented by a combination of four exponential functions. The signal for $W_1=W_2$ is given by [28]:

$$[S(\infty)-S(t)]/S(\infty) = 0.048\exp(-0.476\,W_1t)+0.818\exp(-1.333\,W_1t) + 0.050\exp(-2.381\,W_1t)+0.084\exp(-3.810\,W_1t) \quad (3)$$

where $S(t)$ is the nuclear magnetization at time t. The saturation recovery curves at 300 and 380 K are shown in Fig. 7(a), and the recovery data for these temperatures can be satisfactorily fitted with

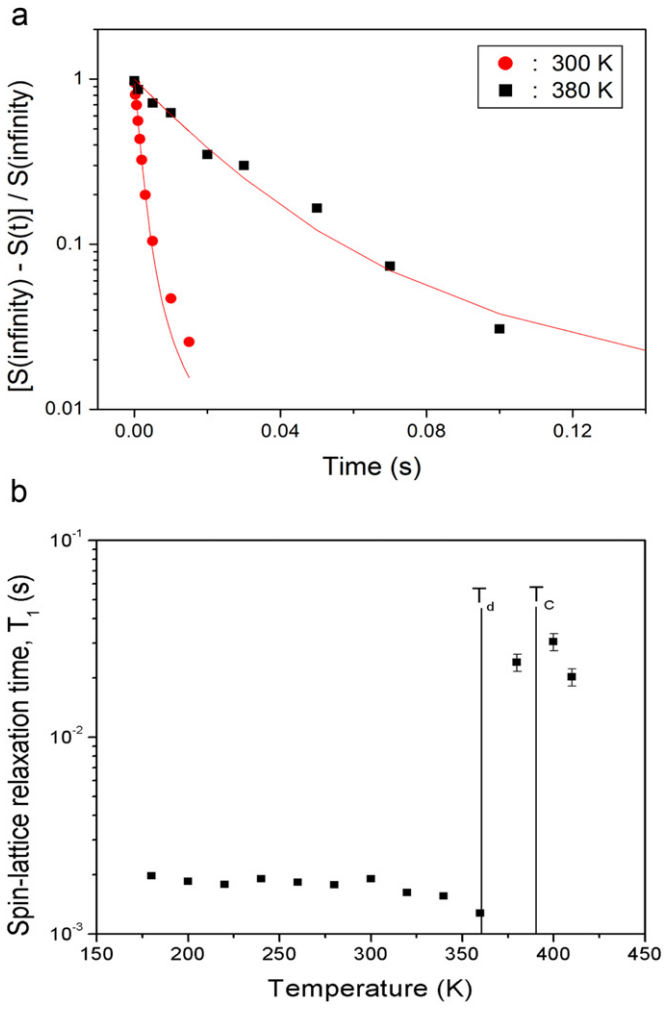

Fig. 7. (a) Recovery traces for ^{133}Cs in a $CsCr(SO_4)_2 \cdot 12H_2O$ single crystal as functions of the delay time and (b) temperature dependence of the spin-lattice relaxation time, T_1, of the ^{133}Cs nucleus in a $CsCr(SO_4)_2 \cdot 12H_2O$ single crystal.

Eq. (3). The recovery trace for the central line of ^{133}Cs in $CsCr(SO_4)_2 \cdot 12H_2O$ crystals can be represented by a combination of four exponential functions. The ^{133}Cs relaxation time was obtained in terms of W_1 ($T_1 = 1/1.333W_1$), and the temperature dependence of the ^{133}Cs spin-lattice relaxation time, T_1, is shown in Fig. 7(b). The relaxation time of the ^{133}Cs nucleus changes abruptly at a temperature that is about 30 K lower than the phase transition temperature 390 K (T_C). This temperature may be consistent with the one set temperature that begins close to 390 K obtained by DSC. Also, the change of the ^{133}Cs T_1 near 360 K is related to the loss of H_2O as shown in the TGA result. The value of T_1 increases abruptly above 360 K, and the changes in ^{133}Cs T_1 at 360 K are the result of transformations of the environments of the Cs^+ atoms. Below 360 K, the ^{133}Cs nucleus in $CsCr(SO_4)_2 \cdot 12H_2O$ has a very short relaxation time of approximately 2 ms [24]. The T_1 values of crystals containing paramagnetic ions are generally shorter than those of crystals without paramagnetic ions [29]. A short T_1 indicates that there is rapid energy transfer from the nuclear spin system to the surrounding environment.

5. Discussion and conclusion

The physical properties and phase transition mechanisms of $RbCr(SO_4)_2 \cdot 12H_2O$ and $CsCr(SO_4)_2 \cdot 12H_2O$ single crystals grown with slow evaporation method were investigated. The decomposition temperatures and phase transition temperatures of $RbCr(SO_4)_2 \cdot 12H_2O$ and $CsCr(SO_4)_2 \cdot 12H_2O$ crystals were determined with NMR, DSC, TGA, and optical polarizing microscopy. The two crystals were found to undergo the loss of H_2O with increases in temperature. And, phase transitions were found to take place at 374 K (T_{C1}) and 425 K (T_{C2}) in the case of $RbCr(SO_4)_2 \cdot 12H_2O$ and at 390 K (T_C) in the case of $CsCr(SO_4)_2 \cdot 12H_2O$. We obtained the NMR spectra of the two crystals and investigated the behaviors of T_1 of the ^{87}Rb and ^{133}Cs nuclei using FT NMR spectroscopy. Above the phase transition temperature, the presence of only one resonance line is due to the structural phase transition; above T_C, the presence of only one M (Rb and Cs) resonance line indicates that the transition is a dynamical averaging of the crystal electric field and M is then apparently in cubic symmetry field. Consequently, the thermal decomposition temperatures (T_d) due to the loss of H_2O in $RbCr(SO_4)_2 \cdot 12H_2O$ and $CsCr(SO_4)_2 \cdot 12H_2O$ crystals, as found in the TGA results, were 330 and 360 K, respectively. These temperatures were consistent with the change from several NMR lines to only one NMR line. And the phase transition temperatures obtained from DSC results was not able to confirm those obtained by NMR experiments. On the other hand, the recovery traces for the central resonance line in case of spin number $I = 3/2,5/2$, and 7/2 can be represented by a combination of two, three, and four exponential functions, respectively [25,26,28]. The recovery traces of the resonance lines of the ^{87}Rb nuclei of $RbCr(SO_4)_2 \cdot 12H_2O$ crystals can each be represented by two single exponential function, whereas that of the central line in the ^{133}Cs nucleus of $CsCr(SO_4)_2 \cdot 12H_2O$ can be represented by a combination of four exponential functions. The relaxation times of the ^{87}Rb and ^{133}Cs nuclei in the two crystals undergo significant changes at a temperature lower than the phase transition temperature. The changes in the temperature dependences of T_1 near the phase transition temperature are related to changes in the symmetry of the octahedra of water molecules about Rb^+ and Cs^+, which are due to the loss of H_2O and mean that the forms of the octahedra of water molecules surrounding Rb^+ and Cs^+ might be disrupted; this transformation is due to the breaking of hydrogen bonds.

We compared these ^{87}Rb and ^{133}Cs NMR results with those obtained for the trivalent cations Cr and Al in $MCr(SO_4)_2 \cdot 12H_2O$ and $MAl(SO_4)_2 \cdot 12H_2O$ crystals. However, the M T_1 values for the $MCr(SO_4)_2 \cdot 12H_2O$ (M=Rb and Cs) crystals are different from those for the $MAl(SO_4)_2 \cdot 12H_2O$ (M=Rb and Cs) crystals [30]. The Cs relaxation time in $CsCr(SO_4)_2 \cdot 12H_2O$ is about 1,000,000 times faster than that in $CsAl(SO_4)_2 \cdot 12H_2O$ at room temperature, whereas the Rb relaxation time in $RbCr(SO_4)_2 \cdot 12H_2O$ is about 1000 times faster than that in $RbAl(SO_4)_2 \cdot 12H_2O$. The T_1 values for the ^{87}Rb and ^{133}Cs nuclei are different due to differences in the local environments of these ions. The differences in T_1 for the two nuclei are due to their different Larmor and quadrupole frequencies amongst other factors. Especially, the influence of the paramagnetic ions is predominant. The spin-lattice relaxation time should be inversely proportional to the square of the quadrupole coupling constant [$1/T_1 \propto (e^2qQ/h)^2$] [31]. The magnitude of the quadrupole coupling constant, e^2qQ/h, for the ^{87}Rb nuclei is of the order of MHz, whereas that of ^{133}Cs nuclei is of the order of kHz. Note that the Cs-based crystals that contain paramagnetic ions exhibit effects that are dominated by their paramagnetic ions, whereas the Rb-based compounds do not; the spin-lattice relaxation times of Cs-based materials with paramagnetic ions are shorter than those of Cs-based crystals without paramagnetic ions, whereas the spin-lattice relaxation times of Rb-based compounds with paramagnetic ions are similar to those of Rb-based crystals without paramagnetic ions [32]. Therefore, the T_1

of crystals containing Cr^{3+} ions is shorter than those of crystals without paramagnetic ions. Cr^{3+} spin dynamics clearly dominate the spin-lattice relaxation behaviors of the Cs-based compounds. Therefore, the ^{87}Rb and ^{133}Cs spin-lattice relaxation is driven by the fluctuations of the magnetic dipole of the Cr^{3+} paramagnetic ions. The temperature dependences of the spin-lattice relaxation times of ^{87}Rb and ^{133}Cs in $RbCr(SO_4)_2 \cdot 12H_2O$, $CsCr(SO_4)_2 \cdot 12H_2O$, $RbAl(SO_4)_2 \cdot 12H_2O$, and $CsAl(SO_4)_2 \cdot 12H_2O$ crystals were compared. The nuclear spin-lattice relaxation times decrease when paramagnetic Cr^{3+} ions are present in place of diamagnetic Al^{3+}. This can be explained by Rb nuclear Cr^{3+} electron spin cross relaxation through interactions consistent with Dionne's [33] measurements on the EPR of Ti^{3+} ($S=1/2$) in Rb alum, where evidence of electron–nuclear spin hyperfine interaction in clearly resolved. Although the quadrupole coupling constants for M (Rb and Cs) and structures of $MCr(SO_4)_2 \cdot 12H_2O$ and $MAl(SO_4)_2 \cdot 12H_2O$ crystals are similar, the T_1 of $MCr(SO_4)_2 \cdot 12H_2O$ are different from those of $MAl(SO_4)_2 \cdot 12H_2O$. Generally, the T_1 values of $MCr(SO_4)_2 \cdot 12H_2O$ crystals, which contains paramagnetic ions, are shorter than those of $MAl(SO_4)_2 \cdot 12H_2O$ crystals. The differences between the trivalent cations Cr and Al are expected to result in differences between the phase transitions of these crystals. Therefore, the relaxation mechanisms of the different types of $M^+Me^{3+}(SO_4)_2 \cdot 12H_2O$ crystals are characterized by completely different NMR behaviors. The $MCr(SO_4)_2 \cdot 12H_2O$ crystals shows different sequences of the structural phase transitions, which may be related to the dynamics and orientation of the octahedron group in the crystal structure.

Acknowledgment

This work was supported by Mid-career Researcher Program through NRF grant funded by the MEST (No. 2010-0000356).

References

[1] S. Radhakrishna, B.V.R. Chowdari, A.K. Viswanath, J. Chem. Phys. 66 (1977) 2009.
[2] R. Bohmer, P. Lunkenheimer, J.K. Vij, I. Svare, J. Phys.: Condens. Matter 2 (1990) 5433.
[3] H. Lipson, C.A. Beevers, Proc. R. Soc. [London] A148 (1935) 664.
[4] A.M. Abdeen, G. Will, W. Schafer, A. Kirfel, M.O. Bargouth, K. Recker, Z.Kristallogr. 157 (1981) 147.
[5] S. Hausuhl, Z. Krist. 116 (1961) 371.
[6] A.H.C. Ledsham, H. Steeple, Acta Cryst. B25 (1969) 398.
[7] G. Cudey, Rev. Chim. Min. 1 (1964) 297.
[8] N. Weiden, A. Weiss, Ber. Bunsenges, Phys. Chem. 78 (1974) 1031.
[9] N. Weiden, A. Weiss, Ber. Bunsenges, Phys. Chem. 79 (1975) 557.
[10] G.F. Dionne, Phys. Rev. A137 (1965) 743.
[11] N. Rumin, Can. J. Phys. 44 (1966) 1387.
[12] V.K. Jain, Physica B 95 (1978) 117.
[13] V.K. Jain, P. Venkateswarlu, Mol. Phys. 36 (1978) 1577.
[14] J.R. Brisson, A. Manogian, J. Magn. Reson. 38 (1980) 215.
[15] S. Dhanuskodi, P. Subramanian, N. Haribaran, Indian J. Phys. 57A (1983) 75.
[16] L. Dubicki, R. Bramley, Chem. Phys. Lett. 272 (1997) 55.
[17] Th. Barthel, F. Wasgestian, J. Lumin. 72-74 (1997) 633.
[18] P.L.W. Tregenna-Piggott, C.J. Noble, J.R. Pilbrow, J. Chem. Phys. 113 (2000) 3289.
[19] B.N. Figgis, P.A. Reynolds, A. Sobolev, Acta Cryst. C56 (2000) 731.
[20] S.P. Best, J.B. Forsyth, J. Chem. Soc. Dalton. Trans. (1991)) .
[21] H.P. Klug, J. Am. Chem. Soc. 62 (1940) 2992.
[22] T. Mildner, H. Ernst, D. Freude, Solid State Nucl. Magn. Reson. 5 (1995) 269.
[23] A.C. Larson, D.T. Cromer, Acta Cryst. 22 (1967) 793.
[24] A.R. Lim, Physica B 405 (2010) 2128.
[25] E.R. Andrew, D.P. Tunstall, Proc. Phys. Soc. 78 (1961) 1.
[26] A. Avogadro, E. Cavelius, D. Muller, J. Petersson, Phys. Status Solidi (b) 44 (1971) 639.
[27] K.H. Kim, D.R. Torgeson, F. Borsa, S.W. Martin, Solid State Ionics 90 (1996) 29.
[28] M. Igarashi, H. Kitagawa, S. Takagawa, R. Yoshizaki, Y. Abe, Z. Naturforsch A47 (1992) 313.
[29] A. Abragam, The Principles of Nuclear Magnetism, Oxford University Press, Oxford, 1961.
[30] A.R. Lim, Solid State Nucl. Magn. Reson. 36 (2009) 45.
[31] R. Bohmer, K.R. Jeffrey, M. Vogel, Prog. Nucl., Magn. Reson. Spectrosc. 50 (2007) 87.
[32] A.R. Lim, J. Appl. Phys. 106 (2009) 93522.
[33] G.F. Dionne, Can. J. Phys. 42 (1964) 2419.